

LA-UR-17-27172

Approved for public release; distribution is unlimited.

Title: MIS High-Purity Plutonium Oxide Metal Oxidation Product TS707001  
(SSR123): Final Report

Author(s): Veirs, Douglas Kirk  
Stroud, Mary Ann  
Berg, John M.  
Narlesky, Joshua Edward  
Worl, Laura Ann  
Martinez, Max A.  
Carillo, Alex

Intended for: Report

Issued: 2017-08-09

---

**Disclaimer:**

Los Alamos National Laboratory, an affirmative action/equal opportunity employer, is operated by the Los Alamos National Security, LLC for the National Nuclear Security Administration of the U.S. Department of Energy under contract DE-AC52-06NA25396. By approving this article, the publisher recognizes that the U.S. Government retains nonexclusive, royalty-free license to publish or reproduce the published form of this contribution, or to allow others to do so, for U.S. Government purposes. Los Alamos National Laboratory requests that the publisher identify this article as work performed under the auspices of the U.S. Department of Energy. Los Alamos National Laboratory strongly supports academic freedom and a researcher's right to publish; as an institution, however, the Laboratory does not endorse the viewpoint of a publication or guarantee its technical correctness.

# MIS High-Purity Plutonium Oxide Metal Oxidation Product TS707001 (SSR123): Final Report

---

## Authors:

D. Kirk Veirs  
Mary A. Stroud  
Max A. Martinez (retired)  
Alex Carillo (retired)  
John M. Berg  
Joshua E. Narlesky  
Laura Worl

# MIS High-Purity Plutonium Oxide Metal Oxidation Product TS707001 (SSR123): Final Report

## Abstract

A high-purity plutonium dioxide material from the Material Identification and Surveillance (MIS) Program inventory has been studied with regard to gas generation and corrosion in a storage environment. Sample TS707001 represents process plutonium oxides from several metal oxidation operations as well as impure and scrap plutonium from Hanford that are currently stored in 3013 containers. After calcination to 950°C, the material contained 86.98% plutonium with no major impurities. This study followed over time, the gas pressure of a sample with nominally 0.5 wt% water in a sealed container with an internal volume scaled to 1/500<sup>th</sup> of the volume of a 3013 container. Gas compositions were measured periodically over a six year period. The maximum observed gas pressure was 138 kPa. The increase over the initial pressure of 80 kPa was primarily due to generation of nitrogen and carbon dioxide gas in the first six months. Hydrogen and oxygen were minor components of the headspace gas. At the completion of the study, the internal components of the sealed container showed signs of corrosion, including pitting.

## Contents

Abstract .....	2
Figures .....	4
Tables .....	5
Introduction .....	6
Material Characerization .....	7
Experimental Procedure .....	10
Results .....	12
Loading.....	12
TGA-MS Results.....	12
Moisture addition .....	13
Gas Generation .....	15
Moisture measurements on unloading.....	16
Corrosion.....	17
Discussion .....	18
Estimation of the amount of moisture on the material during the gas generation study .....	18
The H <sub>2</sub> G-value and rate constants .....	20
Behavior of CO <sub>2</sub> and NO <sub>2</sub> .....	23
Behavior of He .....	24
Conclusions .....	24
Acknowledgements .....	24
References .....	25
Attachment 1: Gas Generation Partial Pressure Data and Uncertainties in kPa .....	26
Attachment 2 Gas Generation: Total Pressure .....	27
Attachment 3 Photographs of the SSR inner bucket .....	30
Appendix 1: Estimating the monolayer coverage .....	34
Appendix 2: Stopping power ratio .....	35

## Figures

Figure 1. TS707001 upon arrival at LANL .....	6
Figure 2. The specific wattage of TS707001 as a function of time from the last measurement date in 1998. The vertical pink lines bound the time the sample was in the reactor.....	9
Figure 3. Integrated amount of He evolved from alpha decay from TS707001 as a function of time and the differential amount of He evolved in 0.1 years as a function of time. The vertical purple lines bound the time the sample was in the reactor. ....	9
Figure 4. Dissassembled SSR: Conflat container body (A) with conflat flange lid (B), copper gasket (C), inner bucket (D), pressure transducer (E), and a sampling volume between two sampling valves with connection to the gas manifold (F). Inner bucket slides into container body and holds the material.....	10
Figure 5. TGA-MS data for the parent material. Mass 17.00 is H <sub>2</sub> O, Mass 30 is NO, and Mass 44.00 is CO <sub>2</sub> . Mass 46 is NO <sub>2</sub> . The cracking pattern of NO <sub>2</sub> in the MS instrument results in mass 30 (NO) as the dominant mass fraction for NO <sub>2</sub> . ....	13
Figure 6. Moisture Addition Curve .....	15
Figure 7. Total pressure and partial pressure of gases measured using a gas chromatograph as a function of time. The error bars are determined from 1 $\sigma$ uncertainties in the total pressure and 1 $\sigma$ uncertainties in the GC sensitivities to the various gases which are determined during the calibration of the GC. ....	15
Figure 8. Corrosion within SSR123 included a) corrosion of the copper gasket, b) pitting of the inner bucket at the top of the headspace region, and c) evidence of liquid at the bottom of the inner bucket. ....	17
Figure 9. Images of the inner bucket after unloading; a) the inner bucket bisected, b) the headspace region showing corrosion in the headspace that stops at the material/gas interface, and c) the bottom of the inner bucket. ....	17
Figure 10. Schematic of an SSR in a heated array. The temperature gradient between the material and the colder plumbing results in moisture moving from the material to cold spots in the plumbing. When the lid is removed during unloading, any moisture condensed in the cold spots will be removed from the system. This moisture is not associated with the material and does not receive alpha radiation dose. Thus, this moisture should not be included in G-value calculations. ....	19
Figure 11. The hydrogen partial pressure and the fit to Equation 1, or zeroth order formation and first order consumption reaction. ....	21

## Tables

Table 1. Material Physical Characteristics .....	7
Table 2. Elemental and isotopic data. Table 2a lists the major elemental constituents measured by analytical chemistry. Table 2b lists soluble elements measured by ion selective electrode or ICP-AES on a leached sample.....	7
Table 3. Isotopic data listed as mass fraction (g/g plutonium). The isotopes were measured on 7-23-1998. ....	8
Table 4. Mass of sample and results of calculation of free gas volume using approach in <i>Obtaining G-values and rate constants from MIS data</i> Appendix A. <sup>6</sup> .....	12
Table 5 . Moisture data summary at loading. ....	14
Table 6. Unloading moisture data summary .....	16
Table 7. The amount of water adsorbed on the material, in the gas phase, and decomposed to form H <sub>2</sub> expressed as moles, grams, and monolayers. The mass of water in a monolayer is 0.00520 g. Calculations use SSA = 2.346 m <sup>2</sup> g <sup>-1</sup> , m <sub>mat</sub> = 10.07 g and V <sub>gas</sub> = 4.439 cm <sup>3</sup> . The amount of chemisorbed water on the material was assumed to be 0.05 wt% at all times. ....	20
Table 8. The fit parameters and standard errors from the hydrogen generation data.....	22
Table 9. G(H <sub>2</sub> ) and rate constants calculated from the reaction parameters and the estimated moisture content using Equations from Reference 6.....	22
Table 10. The amount of carbon and nitrogen species detected on the surface compared to the amount detected in the gas phase. ....	23

## Introduction

The Los Alamos National Laboratory (LANL) Shelf-life Surveillance project was established under the Material Identification and Surveillance (MIS) Program to identify early indications of potential failure mechanisms in 3013 containers.<sup>1</sup> Samples were taken from plutonium processes across the DOE complex. These “representative” materials were sent to LANL to be included in the MIS inventory.<sup>2</sup> The small-scale surveillance project is designed to provide gas generation and corrosion information of the MIS represented materials under worst-case moisture loadings. This information, in combination with material characterization, allows predictions of the behavior of 3013 packaged materials stored at DOE sites. Pressure, gas compositions, and corrosion were monitored in small-scale reactors (SSRs) charged with nominally 10-gram samples of plutonium bearing materials with nominally 0.5 wt% water, the upper limit allowed by the DOE’s 3013 Standard.<sup>1</sup>

This report discusses sample TS707001 (SSR123), a high-purity plutonium dioxide ( $\text{PuO}_2$ ) material from the MIS Program inventory that originated from the thermal stabilization process in Building 707 J-Module at the Rocky Flats Plant (RFETS).<sup>3</sup>

TS707001 is representative of oxides generated from the following processes<sup>2</sup>:

- Metal Oxidation at Hanford
- Impure and Scrap Pu Oxides, 80-85%, from Hanford PFP and 300 Area
- Process Oxides from Metal Oxidation at RFETS
- RFETS oxide from metal oxidation at Savannah River Site (SRS)
- Lawrence Livermore National Laboratory Pu metal burned at SRS
- Oxide from Metal Brushings at SRS
- Metal oxidation at LANL



**Figure 1. TS707001 upon arrival at LANL.**

## Material Characerization

The weapons grade plutonium oxide was calcined at 950 °C for 2 hours on January 21, 1998. Several measurements of material characteristics that were obtained on the calcined sample are summarized in Table 1. Specific power is reported in mW per gram of material, not per gram of plutonium.<sup>4</sup>

**Table 1. Material Physical Characteristics**

Specific Surface Area (SSA) 5-point (m <sup>2</sup> g <sup>-1</sup> )	2.346
Specific Power (mW g <sup>-1</sup> )	2.20
Bulk Density (g cm <sup>-3</sup> )	2.978
Tap Density (g cm <sup>-3</sup> )	3.818
Pycnometer Density (g cm <sup>-3</sup> )	11.3580

Table 2 lists the major elemental constituents of the material. The plutonium facility's analytical chemistry group perfomed the analysis reported in Table 2a using calibrated procedures developed for characterization of plutonium oxide samples. Nitric acid dissolution can result in an undissolved residue which is not reported. Table 2a summarizes the wt% of key elements as well as any impurity present as 0.01 wt% or greater. Oxygen is not measured and it is assumed to make up the difference between the sum of the listed elements plus plutonium and 100%. Table 2b lists the soluble species measured by ion selective electrode (chloride, sodium, potassium, and fluoride) and ICP-AES (calcium, magnesium, chromium, iron, nickel, manganese and molybdenum) present as 0.01 wt% or greater.

**Table 2. Elemental and isotopic data. Table 2a lists the major elemental constituents. Table 2b lists water soluble elements measured by ion selective electrode or ICP-AES on a leached sample.**

Table 2a

Element	wt%
Calcium	< 0.01
Chlorine	0.014
Chromium	0.015
Fluorine	0.085
Gallium	0.060
Iron	0.024
Magnesium	0.0096
Nickel	0.010
Phosphorus	0.034
Potassium	< 0.01
Silicon	0.055
Sodium	< 0.01
Tantalum	0.011
Uranium	0.37

Table 2b

Element	wt%
Calcium	0.024
Chloride	0.036
Fluoride	0.011
Potassium	0.008
Sodium	0.006

Material characterization data from ion chromatography reported in Table 2a indicates 0.014 wt% chlorine while Table 2b reports 0.036 wt% soluble chloride. The as-received material had a chlorine content of 0.19 wt%, which is substantially higher than the 0.014 wt% reported for the calcined material used in SSR123. Material inhomogeneity could result in a low reported chlorine value in Table 2a.

Isotopic Data from calorimetry/gamma isotopics is listed in **Error! Not a valid bookmark self-reference.** Additional material characterization data are published elsewhere.<sup>3, 5</sup>

**Table 3. Isotopic data listed as mass fraction (g/g plutonium). The isotopics were measured on 7-23-1998.**

Isotope	Mass Fraction
Pu-238	0.0001917
Pu-239	0.936993
Pu-240	0.0604745
Pu-241	0.0021845
Pu-242	0.00025
Am-241	0.0015523
Total Plutonium (calorimetry)	0.86975

The specific wattage of TS707001 as a function of time from the 1998 measurement date is shown in **Figure 2**. The specific wattage as a function of time is calculated from the isotopic composition reported in Table 3 using an EXCEL spreadsheet. Input to the spreadsheet includes the half-life<sup>6</sup> and energy per nuclear transition<sup>7</sup> for each isotope. The energy from the uranium decay products are orders of magnitude less than the contribution from the plutonium isotopes over the fifty year time-frame shown in **Figure 2** and are not included in the calculation.

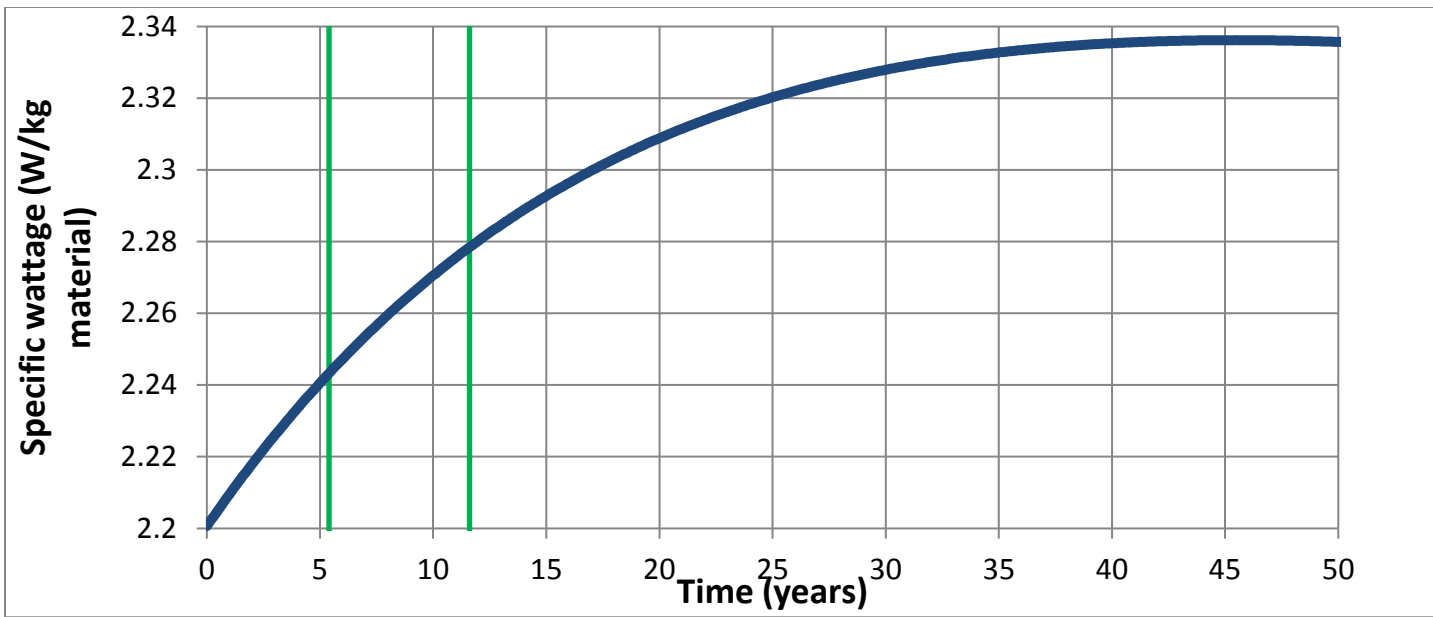


**Figure 2.** The specific wattage of TS707001 as a function of time from the last measurement date in 1998. The vertical green lines bound the time the sample was in the reactor.

The EXCEL spreadsheet used to calculate the wattage also calculates the amount of He produced by alpha decay. This is reported both as the amount of He produced per 0.1 year time increments and the integrated amount of He produced since the time the isotopic fractions were measured. Figure 3 provides information on He evolution as a function of time in TS707001.

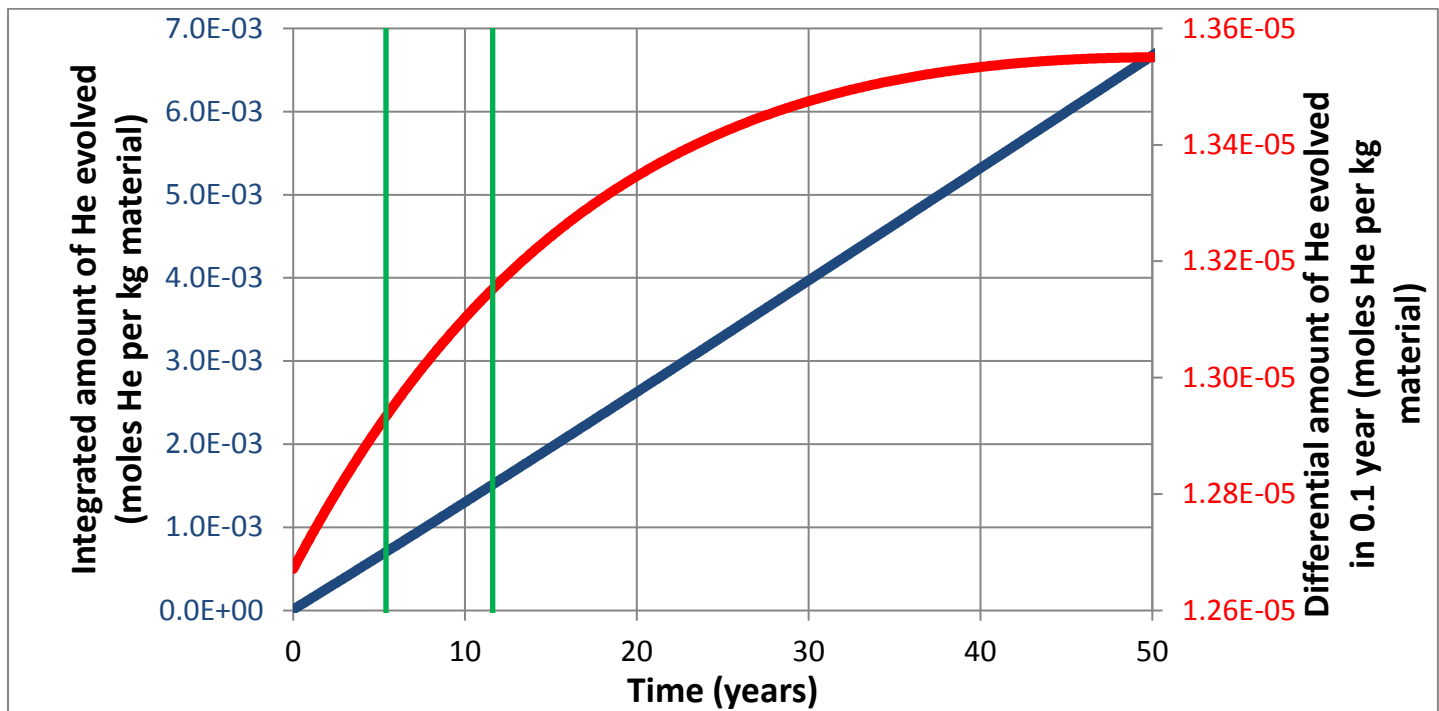


**Figure 3.** Integrated amount of He evolved from alpha decay from TS707001 as a function of time and the differential amount of He evolved in 0.1 years as a function of time. The vertical green lines bound the time the sample was in the reactor.

## Experimental Procedure

Gas composition and pressure of a nominally 10 gram sample is conducted by placing a sample in a small-scale reactor (SSR) and monitoring these parameters over time. Each SSR is given a unique name. The TS707001 material is in reactor SSR123.

The design of the SSR system has been described previously.<sup>8</sup> The assembled reactor's nominally five  $\text{cm}^3$  internal volume is scaled to be  $\sim 1/500^{\text{th}}$  of the inner 3013 storage container. The material of construction of the SSRs is mainly 304L stainless steel. The SSR consists of a container body (called bottom elsewhere<sup>9</sup>) welded into a Conflat flange and a lid consisting of a Conflat flange with tubing attachments for connections to a pressure transducer and a gas manifold. An inner bucket is used to hold material and is inserted into the container body during the loading activities. The inner bucket allows the fine plutonium oxide powder to be handled with minimal or no spillage. A low internal volume pressure transducer and associated low-volume tubing is attached to the lid. Small-scale reactors have interchangeable parts with varying volumes. For this study, a Type H container with a volume of  $5.326 \text{ cm}^3$  without material was used.<sup>9</sup> The gas sampling volume located between two sampling valves,  $0.05 \text{ cm}^3$  ( $\sim 1 \%$  of the SSR volume), allows gas composition to be determined with minimal effect on the internal gas pressure. A disassembled SSR is shown in Figure 4.

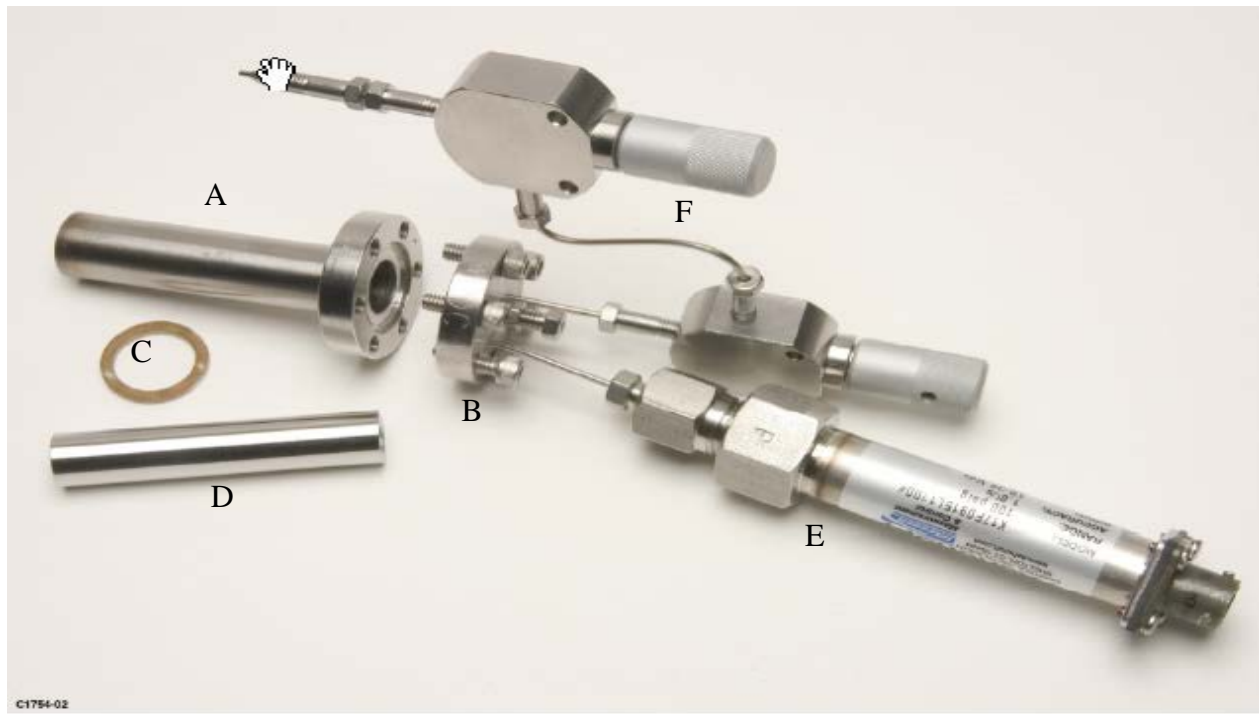


**Figure 4. Dissassembled SSR: Conflat container body (A) with conflat flange lid (B), copper gasket (C), inner bucket (D), pressure transducer (E), and a sampling volume between two sampling valves with connection to the gas manifold (F). Inner bucket slides into container body and holds the mateterial.**

Gas generation is to be characterized for each MIS represented material at the bounding moisture content of 0.5 wt%. The procedure to achieve 0.5 wt% moisture included (1) estimating the moisture content of the material as it was received for small-scale loading and (2) adding sufficient water to bring the total to 0.5 wt%. The moisture content of the material was estimated by weight loss to 200 °C

(LOI-200 °C) of a one gram sample that was cut from the parent lot at the same time as the 10 g small-scale sample. The LOI-200 °C samples were placed in a glass vial which remained in the glove box line with the small-scale sample until the LOI-200 °C measurement was performed, typically one day or less after the sample split and just prior to SSR loading. LOI-200 °C involved heating the sample for 2 hours at 200 °C, cooling for 10 minutes and determining the mass difference of the material before and after heating. The mass loss observed was attributed to adsorbed water volatized by the heating. It was assumed that the LOI-200 °C material contained an additional ~1 monolayer equivalent of water, approximately 0.05 wt%, as hydroxyls or chemically adsorbed water which was not removed by heating to 200 °C.<sup>10</sup> The amount of water to be added to achieve 0.5 wt% total moisture was calculated as the difference between 0.5 wt% and the sum of the adsorbed water determined by LOI-200 °C and the chemically adsorbed water assumed to be 0.05 wt%. In addition, a sample from the parent was split and placed in a glass vial inside of a hermetically sealed container. The water content of this sample was later determined by Thermal Gravimetric Analysis-Mass Spectroscopy (TGA-MS). TGA-MS is inherently more accurate than LOI-200 °C, although there can be errors associated with this method due to handling and excessive times before the sample is run.

The procedure to add moisture is described briefly. A ten-gram sample of the TS707001 material was placed on a balance in a humidified chamber. Weight gain was recorded as a function of time. The sample was then placed into a small-scale reactor and the reactor was sealed as quickly as possible. The glove boxes used for loading and surveillance were flushed with He, resulting in a glove box atmosphere of mainly He with a small amount of air. Some moisture loss was expected during transfer from the humidified chamber into the SSR in the very dry glove box atmosphere (relative humidity < 0.1 %). Transfer time from the balance where the final mass measurement is made to when the SSR was sealed was kept to approximately 45 seconds. Weight loss during transfer for high-purity oxides was measured to be 0.07 wt% per minute.<sup>11</sup> This correction was applied to obtain the estimated moisture content.

The sealed SSR was placed in a heated sample array maintained at 55 °C. Fifty microliter gas samples (~1.1 % of the headspace gas per sample) were extracted through a gas manifold and analyzed using an Agilent 5890 GC (gas chromatograph) calibrated for He, H<sub>2</sub>, N<sub>2</sub>, O<sub>2</sub>, CO<sub>2</sub>, CO and N<sub>2</sub>O. Water vapor was not measured in these samples. The pressure and array temperature was recorded every fifteen minutes. Weekly average pressure values are reported here. Gas composition was sampled at least annually.

At the termination of the experiment, a final GC gas sample was taken, and the SSR was removed from the array and placed in a modified vise which securely holds the SSR when the lid is removed and acts as a heat sink to facilitate temperature equilibration. The SSR lid was removed and a new lid containing a relative humidity sensor was placed on the container. The SSR in the vice was left for a period of time during which the reactor cools and the water vapor equilibrates. The length of time varies and for SSR123 the time was 2 hours and 20 minutes. The relative humidity and temperature in the container were measured using a Vaisala HMT330 sensor and readout. The material was then removed from the container and the moisture content in the material was determined by performing LOI-200 °C.

## Results

### Loading

A ten-gram split from the parent was selected for loading into the SSR. The mass of the sample prior to moisture loading,  $m_{\text{mat}}$ , the volume the material occupies calculated from  $m_{\text{mat}}$  and the pycnometer density,  $V_{\text{mat}}$ , and the calculated free gas volume within the SSR,  $V_{\text{gas}}$ , during the gas generation study are given in Table 4.

**Table 4. Mass of sample and results of calculation of free gas volume using approach in *Obtaining G-values and rate constants from MIS data Appendix A.*<sup>9</sup>**

Mass of sample $m_{\text{mat}}$ (gm)	Volume of Material $V_{\text{mat}}$ (cm <sup>3</sup> )	Volume of SSR $V_{\text{SSR}}$ (cm <sup>3</sup> )	Free Gas Volume in SSR $V_{\text{gas}}$ (cm <sup>3</sup> )
10.07	0.887	5.326	4.439

### TGA-MS Results

TGA-MS data for the sample of the parent material are shown in Figure 5. The sample was split into three subsamples that were analyzed separately. TGA traces for all three subsamples and MS traces for channels that were above background for one of the three samples are illustrated. The majority of the water is released below 200 °C, and is reasonably assigned to physically adsorbed water. A second fraction of water, interpreted to be chemically adsorbed water (hydroxyls) desorbed over a wide range of temperature, extending to above 800 °C.

Nitrogen oxides are the primary volatiles from 200 °C to 400 °C. During the TGA-MS analysis, 0.01 wt% carbon dioxide (~.001g in original sample) and 0.16 wt% nitrogen dioxide was released. Moisture content was determined to be 0.08 wt%. It is evident from these data that the LOI-200 °C loss of 0.17 wt% overestimates the amount of water for this high-purity plutonium dioixde material that had been exposed to air for approximately six years prior to the measurement. The presence of surface adsorbed nitrogen oxide species and CO<sub>2</sub> on aged material limits the accuracy of the LOI-200 °C techniques to estimate water content.

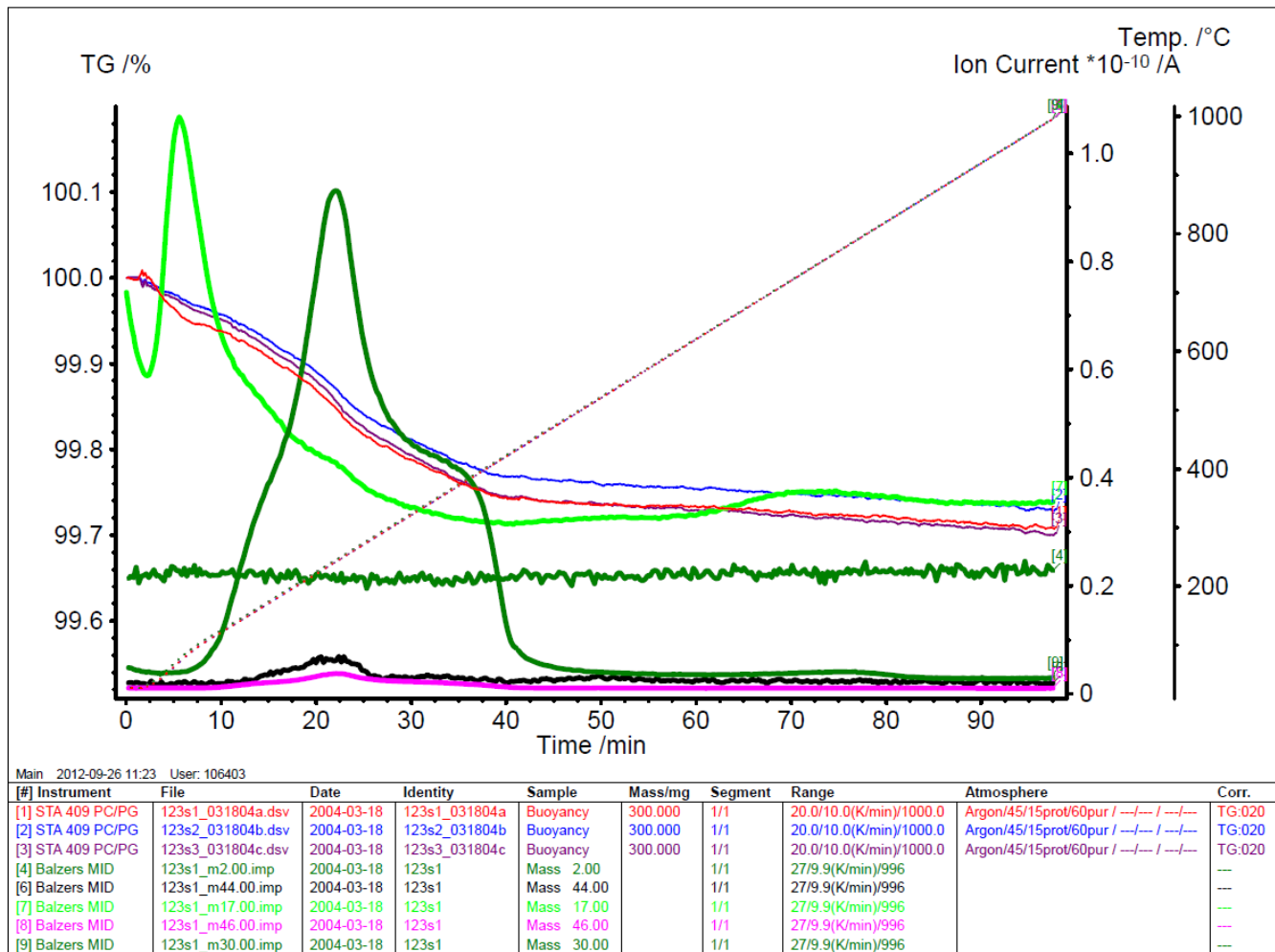


**Figure 5. TGA-MS data for the parent material. Mass 17.00 is H<sub>2</sub>O, Mass 30 is NO, and Mass 44.00 is CO<sub>2</sub>. Mass 46 is NO<sub>2</sub>. The cracking pattern of NO<sub>2</sub> in the MS instrument results in mass 30 (NO) as the dominant mass fraction for NO<sub>2</sub>.**

### Moisture addition

The measurements taken at the time of loading are summarized in Table 5. The moisture present initially in the material was estimated from the LOI-200 °C and chemisorbed moisture to be 0.22 wt%. The TGA-MS measurement of the initial moisture was 0.08 wt%. The significant difference of 0.14 wt% arose from the large amount of NO<sub>x</sub> and to a lesser extent CO<sub>2</sub> that came off the material before 200 °C as seen in the TGA-MS, Figure 5. The best value for the moisture content at loading is 0.27 wt% as given in Table 5 line 12, Estimated Total Moisture in loaded sample (using TGA-MS).

**Table 5 . Moisture data summary at loading.**

	Parameter	Value	Units
1	Original Calcination Date	1/21/1998	
2	Loading Date	12/16/2003	
3	Unloading Date	3/2/2010	
4	Initial sample weight (m <sub>mat</sub> )	10.07	g
5	Initial Moisture (Total) by TGA-MS	0.08	wt%
6	Initial Moisture by LOI-200 °C	0.17	wt%
7	Estimated additional (chemisorbed) moisture present	0.05	wt%
8	Total Moisture added	0.24	wt%
9	Relative Humidity in glove box during loading	0.1/24.8	% / °C
10	Estimated moisture loss during loading	0.05	wt%
11	Estimated Total Moisture in loaded sample (using LOI) = Line 6 + Line7 +Line8 -Line 10	0.41	wt%
12	Estimated Total Moisture in loaded sample (using TGA-MS) = Line 5 + Line 8 -Line 10	0.27	wt%

Two analytical balances were used during moisture uptake. One analytical balance was configured with a dish of water to raise the RH within the balance chamber where the sample sits. The dish of water could be heated if necessary to achieve a RH near saturation. The balance chamber was partially sealed with tape to prevent moisture escaping. The RH within the chamber was raised with respect to the glovebox atmosphere, but did not reach equilibrium. Moisture uptake to 0.5 wt% for high-purity plutonium oxides with specific surface areas less than  $\sim 5 \text{ m}^2 \text{ g}^{-1}$  such as TS707001 requires a RH near saturation because many monolayers need to condense on the sample. The RH within the balance during moisture uptake was high, i.e. greater than 25% RH and up to 90% RH if the water was heated, but was not measured for SSR123. The second analytical balance was used for a final measurement of the mass of the sample. The second balance was necessary because the configuration and atmosphere within the first balance prevents calibration. The moisture uptake as a function of exposure time for SSR123 is plotted in Figure 6. The increase in mass is attributed to water adsorption by the material. Some loss of water occurs between when the material is transferred from the humidified chamber to the balance where the final mass measurement is made. Thus, the total moisture added in Table 5, 0.24 wt%, does not exactly match the mass gain during moisture uptake 0.26 wt%.

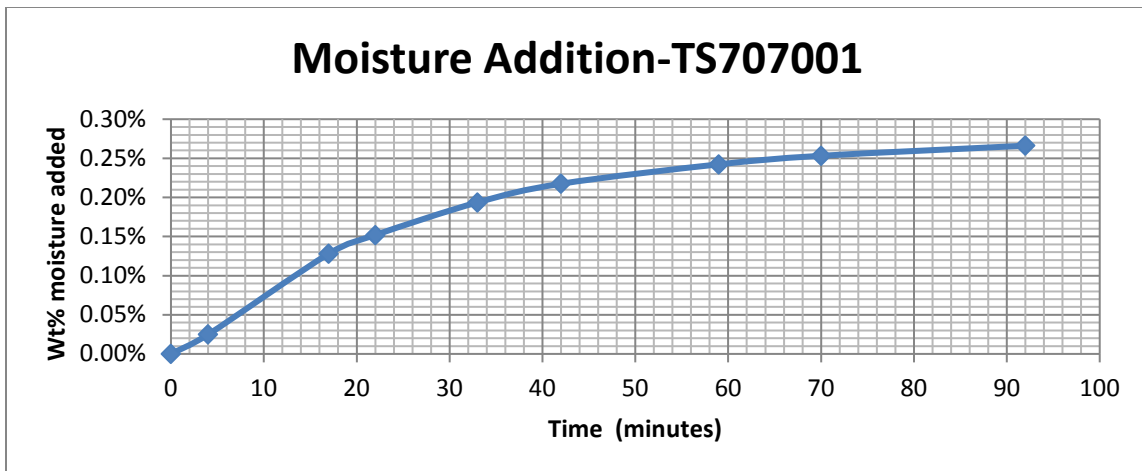


**Figure 6. Moisture Addition Curve**

### Gas Generation

The total pressure in SSR123 as a function of time, as well as the partial pressure of several gasses, is shown in Figure 7. Detailed information on gas composition and uncertainties is in Attachment 1 and on pressure in Attachment 2.

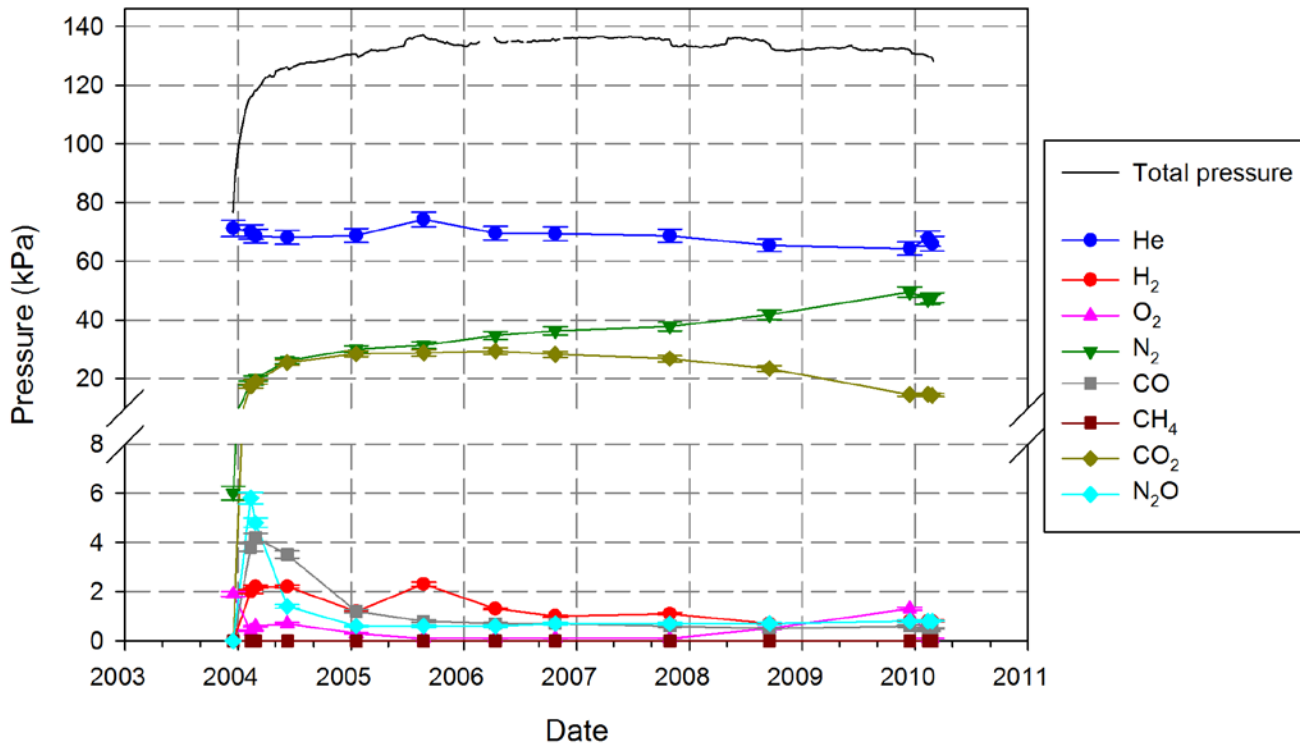


**Figure 7. Total pressure and partial pressure of gases measured using a gas chromatograph as a function of time. The error bars are determined from  $1\sigma$  uncertainties in the total pressure and  $1\sigma$  uncertainties in the GC sensitivities to the various gases which are determined during the calibration of the GC.**

The initial pressure of 78 kPa increased to 125 kPa in the first three months and gradually increased to a maximum pressure of 137 kPa over the next 17 months. The initial 78 kPa pressure was measured when SSR123 was still at room temperature, 25 °C. Based on the ideal gas law, it is expected that the pressure rose rapidly to 86 kPa due to the increase in SSR123 temperature to 55 °C when it was placed in the heated array. Hydrogen and oxygen were minor components in the headspace gas. Hydrogen was initially not detected and increased to close to its maximum observed partial pressure of 2.3 kPa within 7 weeks. Hydrogen persisted at this level for roughly two years before it slowly decreased to an apparent steady-state value of 0.8 kPa. Oxygen began at 1.9 kPa and decreased to about 0.5 kPa within seven weeks and then to 0.1 kPa within two years where it remained for approximately 2 years.

Over the next sixteen month time range, September 2008 to December 2009, the measured oxygen partial pressure rose to 1.3 kPa before returning to 0.1 kPa for the last measurement. The nitrogen partial pressure also increased and then decreased for the last measurement. These observations are assumed to be due to insufficient pump down/air leakage during sampling.

The net increase in total pressure during the experiment was primarily due to the generation of nitrogen and carbon dioxide. Initially carbon monoxide and nitrous oxide were generated to a maximum pressure of near 5 kPa and then decreased to less than 1 kPa. There was little change in the total pressure within the container over the final four years though the amount of nitrogen continued to increase while the amount of carbon dioxide decreased with time.

### **Moisture measurements on unloading**

The SSR was removed from the heated array on March 2, 2010 and placed in a holder to cool. While the SSR was still warm the lid was removed and replaced with a lid modified to hold a RH sensor. The relative humidity and temperature in the container were measured using a Vaisala HMT330 sensor and readout. The moisture content in the material at termination was determined by performing LOI-200 °C, which showed 0.10 wt% loss, and adding an additional 0.05 wt% to account for chemically adsorbed water that was not removed by heating to 200 °C. Other adsorbed gases may also desorb at 200 °C (see explanation under moisture at loading), so the LOI-200 °C value is expected to be high. Sample loading, unloading and moisture data are summarized in Table 6.

**Table 6. Unloading moisture data summary**

	Parameter	Value	Units
1	Unloading Moisture by LOI-200 °C	0.10	wt%
2	Estimated additional (chemisorbed) moisture present	0.05	wt%
3	Estimated total moisture at unloading = Line 1 + Line 2	0.15	wt%
4	Relative Humidity/Temperature in headspace at unloading	26 / 23.5	% / °C
5	Number of monolayers at unloading RH and temperature using Figure A-1.	0.9 – 1.3	ML
6	Mass of physisorbed water using average of line 5.	0.06	wt%
7	Estimated total moisture at unloading from RH and temperature = line 2 + line 6	0.11	wt%

## Corrosion

Corrosion was observed within SSR123, which was unexpected because the material is high-purity plutonium dioxide with only trace amounts of chlorine. Corrosion was observed in the headspace

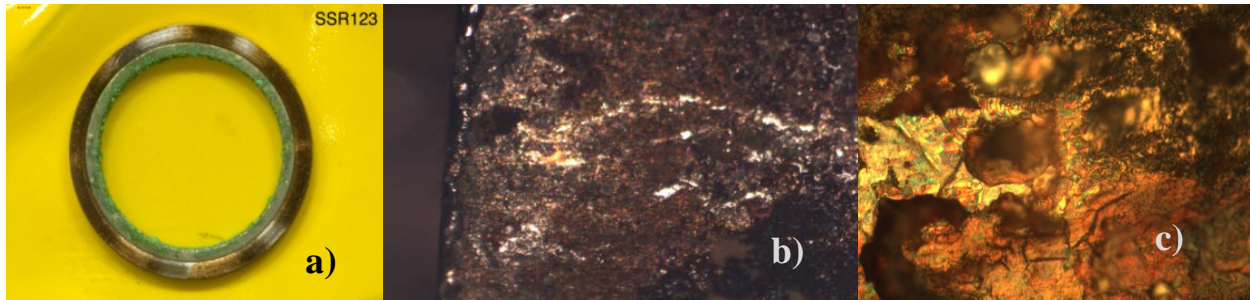


**Figure 9. Corrosion within SSR123 included a) corrosion of the copper gasket, b) pitting of the inner bucket at the top of the headspace region, and c) evidence of liquid at the bottom of the inner bucket.**

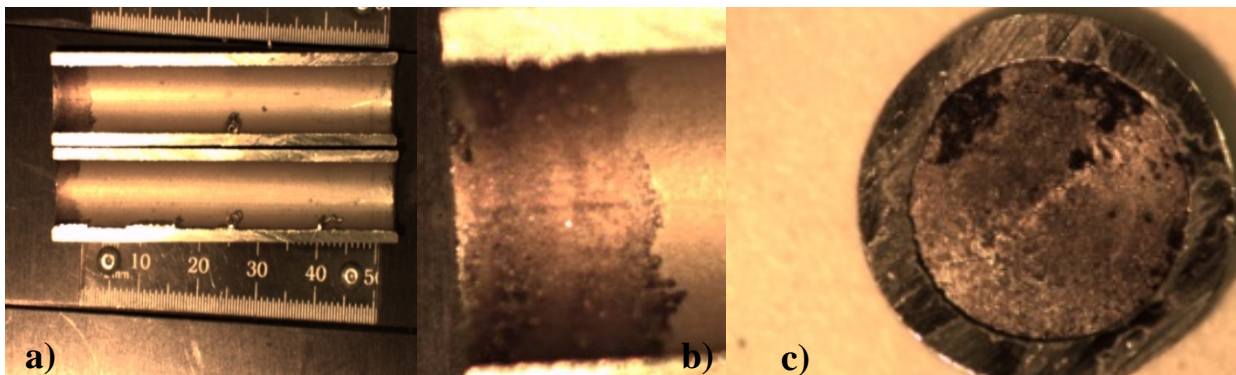


**Figure 8. Images of the inner bucket after unloading; a) the inner bucket bisected, b) the headspace region showing corrosion in the headspace that stops at the material/gas interface, and c) the bottom of the inner bucket.**

region and in the bottom of the inner bucket, Figure 8. Corrosion in the headspace region included visible corrosion of the copper metal gasket and pitting on the inner bucket. Other corrosion evidence included observation of a brown residue at the bottom of the inner bucket, Figure 9.

Additional pictures of the corrosion are in Attachment 3. The dried residue appeared to result from a liquid formed during corrosion. The green coating observed on the copper gasket was scraped and 3.7 mg of green "powder" was recovered. Scrapings of the powder were dissolved in 0.1M nitric acid and tested with chloride strips. The solution tested positive for chloride however the high pH of the solution may have affected the measurement. X-Ray Diffraction analysis of the powder identified only copper as a component. C-AAC identified XRD peaks for CuCl from that same material. With the limited data available, the compound was not definitively identified. It may be a form of copper (II) chloride that is green when hydrated. Assuming the compound is CuCl<sub>2</sub> dihydrate, 3.7 mg would contain 1.5 mg of chloride.

The corrosion of the copper gasket and the inner bucket in the headspace is evidence that gas-phase corrosive species containing chlorine were evolved from the material.

## Discussion

A goal of the small-scale surveillance studies is to understand the hydrogen gas generation response of material exposed to moisture over a broad range of materials. Recommendations on the analysis of hydrogen partial pressure curves include calculations to obtain hydrogen G-values and formation and consumption rate constants assuming that the hydrogen gas is formed either from radiolysis or from surface decomposition of water.<sup>9</sup> In order to perform these calculations, knowledge of the moisture content of the material during the study and the radiation dose to the moisture is required. We will first discuss the amount of moisture on the material during the study and use the results as input to the  $G(H_2)$  and rate constant calculations. We will follow those results with a discussion of the observation of other gases.

Unlike plutonium-bearing materials currently stored in 3013 containers throughout the DOE complex, TS707001 was exposed to the glove box environment for nearly six years between calcination and loading into the SSR. A significant formation of hydroxyls on the oxide surface is expected after this much time. Gases, such as carbon dioxide or NO<sub>x</sub>, would also be physically adsorbed to the surface and come off of the material when moisture is added to the system, possibly explaining the in-growth of these gases in the headspace as seen in Figure 7. The presence of these species may alter the gas generation behavior compared with recently calcined plutonium oxide. These parameters are summarized in Table 7 along with the amount of moisture associated with the material which is discussed below.

### Estimation of the amount of moisture on the material during the gas generation study

Moisture adsorbed on high-purity plutonium dioxide such as TS707001 is thought to exist as physisorbed water that behaves according to BET theory<sup>12</sup> and as chemically bound water with very low chemical activity (very low water vapor pressure). The latter water can be described as surface hydroxyls and is removed from the plutonium dioxide surface only at high temperatures. In order to use BET theory to estimate the amount of water on the material during the experiment, the SSA, the amount of water in a monolayer, and the amount of water in the gas phase at 100% RH are needed.

The difference between the best estimate of the amount of water in the reactor when the material was loaded and the amount of water estimated to be on the material when the sample was unloaded, .0121 g ([Table 5: line 12 – Table 6: line 3] \*10g), is much greater than the amount of water that produced H<sub>2</sub> plus the amount of water that would be in the gas phase at unloading, 0.00009 g. This suggests that there is a sink for water that has not been identified. An explanation is shown schematically in Figure 10. The material had 5.2 monolayers of water on the surface at loading, of which approximately 1 monolayer equivalent is thought to be chemisorbed water. The remaining ~4.2 monolayers of physisorbed water is in equilibrium with water vapor. According to BET theory, Appendix 1, 4.2 monolayers of physisorbed water would be in equilibrium with an atmospheric water vapor content of ~75% RH. When the SSR is placed in the array, the material temperature is raised to 55 °C. To maintain the 75% RH equilibrium with the warmer material, the water vapor pressure increases to  $0.75 \times 15.752 \text{ kPa} = \sim 12 \text{ kPa}$ . This water vapor pressure exceeds the saturated water vapor pressure at the coldest spot in the system which is 4.24 kPa at ~30 °C. Water condenses in the colder region until the water vapor pressure reaches the condensation pressure of 4.24 kPa. The RH above the material which is at 55 °C is  $4.24/15.572 \times 100\% = \sim 25\%$  (Appendix 1 discusses the monolayer vs RH relationship). At this RH approximately 1.1 monolayers of physisorbed water is on the surface. When the lid is removed at unloading and replaced with the modified lid containing the

RH sensor, the water that is condensed in the plumbing is removed from the system. During the ~6 years of the gas generation study, the moisture in the cold region is located at a sufficient distance from the material that it will receive a radiation dose mainly from gamma radiation. This dose is orders of magnitude smaller than the dose the water associated with the material receives. Thus, this water should not be included in G-value calculations.

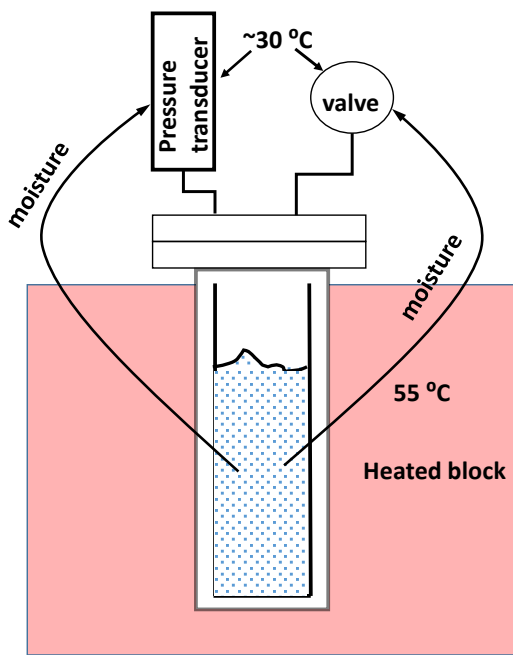


**Figure 10. Schematic of an SSR in a heated array. The temperature gradient between the material and the colder plumbing results in moisture moving from the material to cold spots in the plumbing. When the lid is removed during unloading, any moisture condensed in the cold spots will be removed from the system. This moisture is not associated with the material and does not receive alpha radiation dose. Thus, this moisture should not be included in G-value calculations.**

While the mechanism of the adsorption of water onto plutonium oxide is not well understood, it is believed that hydroxyls form upon initial exposure to water.<sup>13</sup> LOI-200 °C measurements do not detect strongly bound chemisorbed water such as hydroxyls. A gradual conversion of physisorbed water to chemisorbed water (hydroxyls) during the experiment would also contribute to lower measured moisture content at the termination of the experiment than at the beginning because more water would be inaccessible to the LOI-200 °C measurement. The conversion of weakly-bound water to strongly-bound water over time for recently calcined pure plutonium oxide material loaded in similar reactors with relative humidity varying from 30-80 % was observed in the range of 0.3 to 1.0 monolayers of water within 180 days, which corresponds to approximately 0.02 to 0.05 wt% for this sample, much less than the difference between the moisture at loading and unloading.<sup>14</sup>

Given the measured RH of 26% at 23.5 °C in the SSR at unloading, BET theory predicts 0.9 to 1.3 (average 1.1) ML or 0.06 wt% physisorbed water was present and assuming 1 ML or 0.05 wt% present as chemisorbed water, the best estimate of the moisture at unloading is 0.11 wt% .

Table 7 summarizes the amount of water on the material, in the gas phase, and decomposed to form H<sub>2</sub> expressed as weight percent, moles, grams, and monolayers.

**Table 7. The amount of water adsorbed on the material, in the gas phase, and decomposed to form H<sub>2</sub> expressed as moles, grams, and monolayers. The mass of water in a monolayer is 0.00520 g. Calculations use SSA = 2.346 m<sup>2</sup> g<sup>-1</sup>, m<sub>mat</sub> = 10.07 g and V<sub>gas</sub> = 4.439 cm<sup>3</sup>. The amount of chemisorbed water on the material was assumed to be 0.05 wt% at all times.**

Condition	Amount of Water			
	wt%	g	moles	monolayers
	0.052	0.00520	0.000289	1
In gas at 25 °C and 100% RH (3.169 kPa)		9.29x10 <sup>-5</sup>	5.16x10 <sup>-6</sup>	0.018 (equivalent)
In gas at 55 °C and 100% RH (15.75 kPa)		4.62x10 <sup>-4</sup>	2.56x10 <sup>-5</sup>	0.089 (equivalent)
In gas at unloading, 24 °C and 25% RH (0.746 kPa)		2.19 x10 <sup>-5</sup>	1.21x10 <sup>-6</sup>	0.00042 (equivalent)
Reacted to produce max H <sub>2</sub> in gas at 55 °C (2.2 kPa)	6.4 x10 <sup>-4</sup>	6.5x10 <sup>-5</sup>	3.6x10 <sup>-6</sup>	0.012 (equivalent)
On material at loading: physi+chemisorbed	0.27	0.027	1.5x10 <sup>-3</sup>	5.2
On material at unloading: physi+chemisorbed	0.11	0.011	6.2x10 <sup>-4</sup>	2.1
Inferred condensed on piping at 25 °C (the difference of the two preceding lines)	0.16	0.016	8.9x10 <sup>-4</sup>	3.1
On material at unloading: physisorbed	0.06	0.006	3.3x10 <sup>-4</sup>	1.2

### The H<sub>2</sub> G-value and rate constants

It is recommended that  $G(H_2)$  and rate constants be calculated for materials where H<sub>2</sub> is observed. The mathematical formalism is given in *Obtaining G-values and rate constants from MIS data*.<sup>9</sup> First, the hydrogen partial pressure versus time observations are fit to a single exponential function. The initial H<sub>2</sub> generation rate is determined from the four measurements of hydrogen partial pressure taken over the first 200 days of the experiment (Figure 7). The results are given in Table 8.

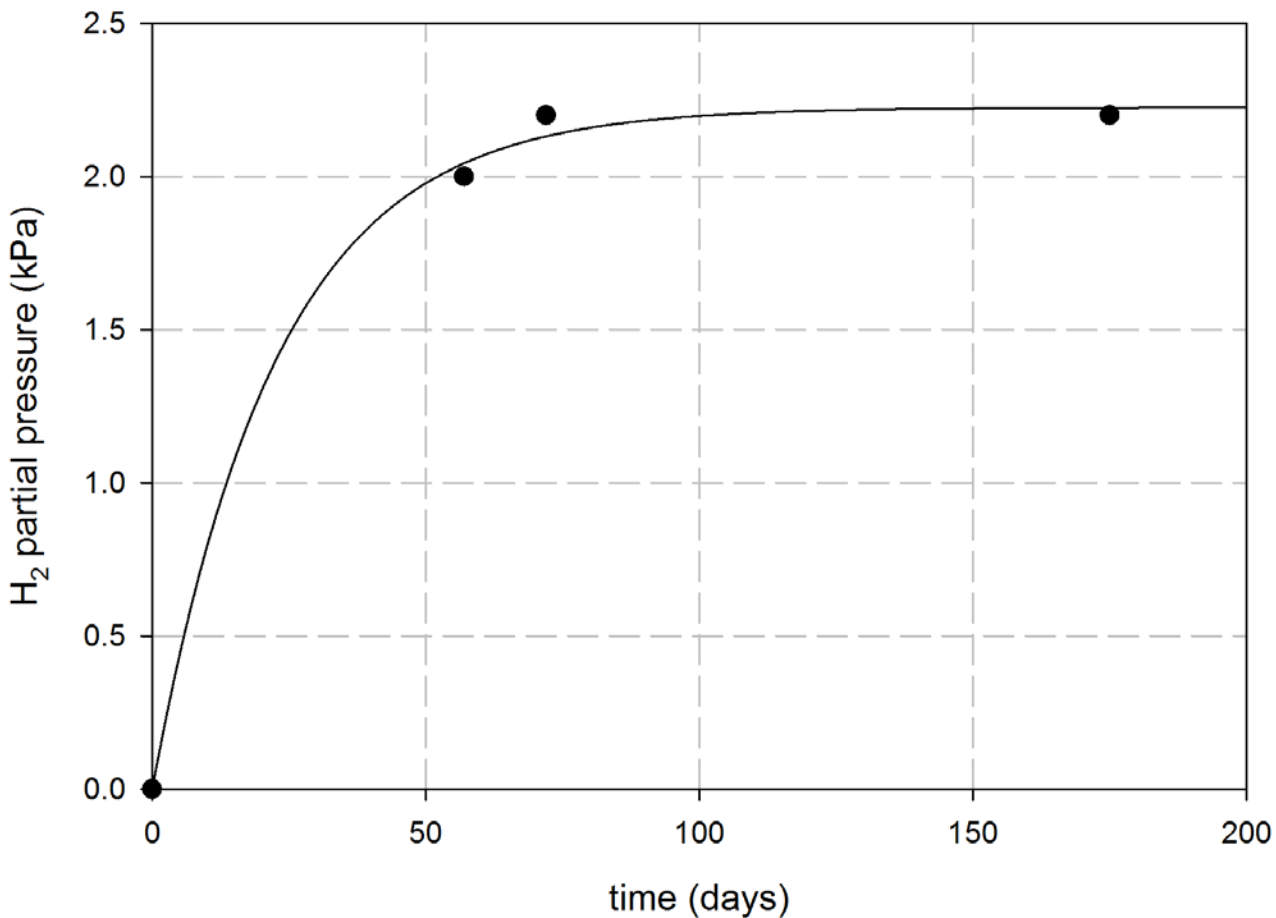


**Figure 11. The hydrogen partial pressure and the fit to Equation 1, or zeroth order formation and first order consumption reaction.**

The H<sub>2</sub> partial pressure increased by 2.0 kPa the first 57 days, indicating a lower limit for the initial production rate of 0.035 kPa/day or  $3.0 \times 10^{16}$  molecules/day. The pressure of H<sub>2</sub> then reached a steady state of 2.2 kPa by day 70. The hydrogen gas generation rate was determined by fitting the hydrogen partial pressure data to Equation 1 which expresses H<sub>2</sub> pressure as a function of time,

$$p = a(1 - e^{-bt}) \quad \text{Equation 1}$$

where  $a$  has units of kPa and  $b$  has units of day<sup>-1</sup>. Detailed information on the derivation of the equation and interpretation of the fit parameters may be found elsewhere.<sup>6</sup>

The values for the fit parameters yielding the curves in **Figure 11** along with the standard error in the parameters are given in **Table 8**. We will use these values to calculate  $G(H_2)$  and the rate of the hydrogen consumption reactions.

**Table 8. The fit parameters and standard errors from the hydrogen generation data.**

Small-scale Surveillance sample identification	$a = k_1/k_2 = P_{max}$ (kPa)	standard error (kPa)	$b = k_2$ (day <sup>-1</sup> )	standard error (day <sup>-1</sup> )
SSR123	2.23	0.06	0.044	0.008

The fitting constants are used to calculate  $G(H_2)$  and reaction rate constants for four different ways of estimating the moisture subjected to radiation dose,  $m_{H_2O}$ : 1) the total water mass at loading (which is not representative of the water physically present on the material during the experiment), 2) the mass of water associated with the  $H_2$  gas pressure, 3) the mass associated with the physisorbed water at unloading, and 4) the mass associated with both the chemisorbed and physisorbed water at unloading. The stopping power ratio is 3.70.

**Table 9.  $G(H_2)$  and rate constants calculated from the reaction parameters and the estimated moisture content using Equations from Reference 6.**

TS707001				
Variable	$m_{H_2O}$	Equation in Ref 6	Value	Units
$G(H_2)$ from water at loading (physisorbed+chemisorbed)	$2.7 \times 10^{-2}$ g	6	0.079	molecules $100\text{eV}^{-1}$
$G(H_2)$ from $H_2$ max pressure	N/A	8	33	molecules $100\text{eV}^{-1}$
$G(H_2)$ from RH at unloading (physisorbed)	$6.0 \times 10^{-3}$ g	6	0.36	molecules $100\text{eV}^{-1}$
$G(H_2)$ from water at unloading (physisorbed+chemisorbed)	$1.1 \times 10^{-2}$ g	6	0.19	molecules $100\text{eV}^{-1}$
$k_1$	--	10	$1.1\text{E+12}$	molecules $\text{s}^{-1}$
$k_2$	--	10	$5.0\text{E+11}$	molecules $\text{s}^{-1} \text{kPa}^{-1}$
$R_{for}$	--	12	0.28	nanomoles $\text{m}^{-2} \text{hr}^{-1}$
$R_{con}$	--	13	0.13	nanomoles $\text{m}^{-2} \text{hr}^{-1} \text{kPa}^{-1}$

Figure 12 compares the  $G(H_2)$  values determined in this study with those reported previously.<sup>15</sup>

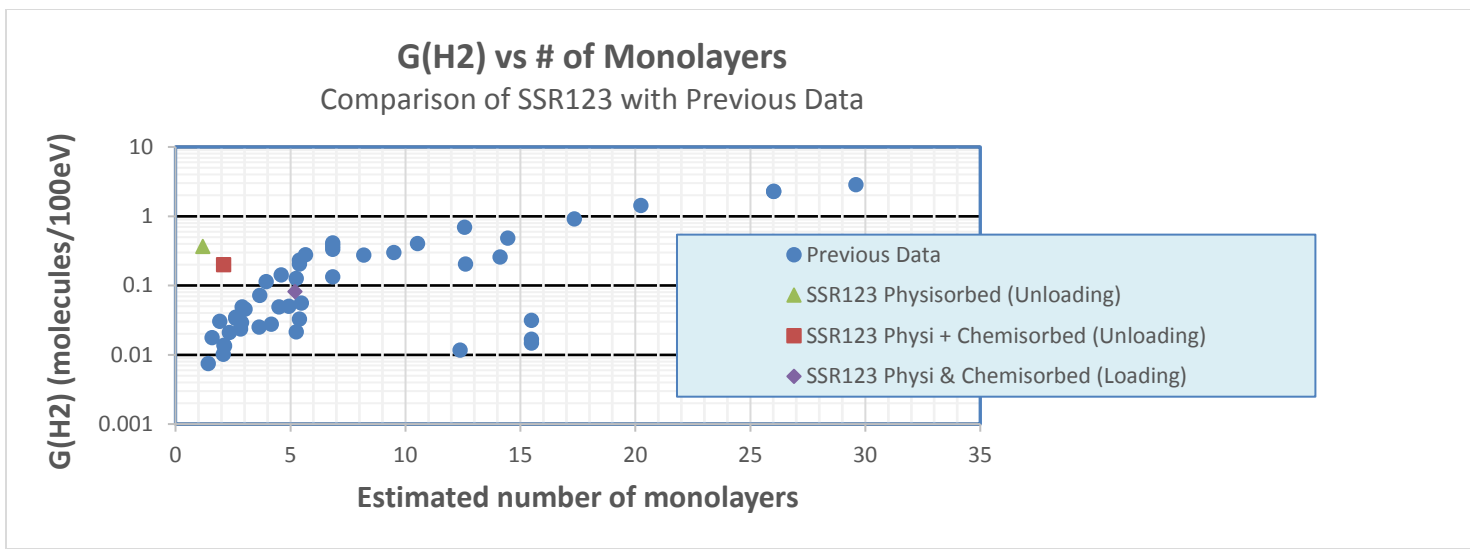


**Figure 12** Comparison of calculated  $G(H_2)$  plotted against the number of calculated water monolayers determined in this study with those from previous research.<sup>15</sup>

### Behavior of CO<sub>2</sub> and NO<sub>2</sub>

The carbon dioxide and nitrogen dioxide detected by TGA-MS on the 10 g sample at loading are a possible source for the CO<sub>2</sub> and N<sub>2</sub> observed in the gas phase. (The compounds actually bound to plutonium dioxide surface could have been any of the general forms CO<sub>x</sub> and NO<sub>x</sub>). The number of moles of nitrogen gas and carbon dioxide present in the head space at the termination of the experiment were calculated using the ideal gas law,  $n = PV/RT$ , where  $V = 4.44 \text{ cm}^3$ ,  $T = 328 \text{ K}$ , and  $P$  = partial pressure of the gas ( $P_{CO_2} = 14 \text{ kPa}$  at termination and 29 kPa at maximum detected and  $P_{N_2} = 49 \text{ kPa}$  at termination which was also the maximum). Results are summarized in Table .

**Table 10.** The amount of carbon and nitrogen species detected on the surface compared to the amount detected in the gas phase.

	CO <sub>2</sub> (moles)	NO <sub>2</sub> (moles)	N <sub>2</sub> (moles)	N (moles)
Sample (Loading-TGA-MS)	$2 \times 10^{-5}$	$3.5 \times 10^{-4}$	Not measured	$3.5 \times 10^{-4}$
Head Space (Termination-GC)	$2 \times 10^{-5}$	Not measured	$8 \times 10^{-5}$	$1.6 \times 10^{-4}$
Max Detected in Head Space over duration of experiment (GC)	$5 \times 10^{-5}$	Not measured	$8 \times 10^{-5}$	$1.6 \times 10^{-4}$

Twice as much carbon dioxide was released as was detected by TGA-MS, and approximately half as much elemental nitrogen was released into the headspace as N<sub>2</sub> as was desorbed as NO<sub>x</sub> gases detected by TGA-MS. Prior to loading the sample in the small-scale reactor, the plutonium dioxide powder was exposed to air for six years (nitrogen and oxygen with small amounts of water and carbon dioxide). Then the sample was placed in a helium atmosphere within the small-scale reactor with a large partial pressure of water. A possible explanation for

the increase in CO<sub>2</sub> is that the water displaced chemically adsorbed CO<sub>2</sub> from the surface sites. The excess CO<sub>2</sub> over the TGA-MS measurement is not explained. The production of N<sub>2</sub> from the NO<sub>x</sub> species adsorbed on the surface suggests that the reaction to form NO<sub>x</sub> from radiolysis of air is reversible in the alpha radiation environment on the surface.

### **Behavior of He**

The alpha decay of the Pu and Am creates He, which may escape the oxide into the gas phase. The amount of He created depends upon the mass of the material and the rate of decay of the various isotopes. The rate of decay can be illustrated graphically as the specific wattage calculated from the reported isotopes, Figure 2. Results were calculated using the last reported isotopes measurements taken on July 23, 1998 that are reported in Table 3. The integrated and differential amount of He evolved as a function of time are shown in Figure 3.

The amount of He created due to alpha decay over the time the material was in the SSR is estimated to be  $8.3 \times 10^{-6}$  moles for the 10 g sample. This amount of He would result in a gas pressure increase of 5.1 kPa in the 4.439 ml of gas volume and gas temperature of 328 K, if all the He was released into the gas phase. The data show the He pressure declined by a net amount of 5.2 kPa. Gas sampling should have resulted in a decline of 8.1 kPa over the course of the study. The difference of 2.9 kPa He added to the gas phase indicates that ~55% of the He from alpha decay was released into the gas phase. This analysis does not account for any leaks in the system or the large uncertainties (see Attachment 1) associated with the He gas measurements.

### **Conclusions**

The MIS item TS707001 was entered into surveillance in December, 2003 and removed from surveillance in August of 2009. The amount of water on the material during the gas generation study was estimated to be 0.11 wt%. The gas generation was dominated by N<sub>2</sub> and CO<sub>2</sub>. Hydrogen was initially generated to a maximum partial pressure of 2.2 kPa and then decreased to an equilibrium value of approximately 1.0 kPa. The oxygen that was initially present was mainly consumed and a partial pressure of approximately 0.1 kPa seemed to be the final equilibrium value. Corrosion was observed in the headspace that appears to be due to a corrosive chlorine containing gas. Corrosion was also observed in the material phase.

### **Acknowledgements**

Funding for this work was provided to the MIS Program by the Assistant Manager for Nuclear Materials Stabilization, Savannah River Operations Office, of the Department of Energy's Office of Environmental Management.

## References

1. U. S. Department of Energy, Stabilization, Packaging, and Storage of Plutonium-Bearing Materials. U.S. Department of Energy: Washington, D.C., 2012.
2. Narlesky, J. E.; Peppers, L. G.; Friday, G. P. *Complex-Wide Representation of Material Packaged in 3013 Containers*; LA-UR-14396; Los Alamos National Laboratory: Los Alamos, NM, 2009.
3. Toupadakis, A.; Davis, C.; Foster, L.; Horrell, D. R.; Mason, R.; Trujillo, J. *Materials Identification and Surveillance Project Item Evaluation Item: Impure Plutonium Oxide (TS707001)*; LA-UR-98-1137; Los Alamos National Laboratory: Los Alamos, NM, 1998.
4. Narlesky, J. E.; Stroud, M. A.; Smith, P. H.; Wayne, D. M.; Mason, R. E.; Worl, L. A. *Characterization of Representative Materials in Support of Safe, Long Term Storage of Surplus Plutonium in DOE-STD-3013 Containers*; LA-UR-12-23790; Los Alamos National Laboratory: Los Alamos, NM, 2012.
5. Narlesky, J. E. S., M. A.; Smith, P. H.; Wayne, D. M.; Mason, R. E.; Worl, L. A. *Characterization of Representative Materials in Support of Safe, Long Term Storage of Surplus Plutonium in DOE-STD-3013 Containers*; LA-UR-12-23790; Los Alamos National Laboratory: Los Alamos, NM, 2012.
6. Ahmad, I., Appendix II. Nuclear Properties of Actinide and Transactinide Nuclides. In *The Chemistry of the Actinide and Transactinide Elements*, Springer: Dordrecht, Netherlands, 2007; Vol. 5, p 3442.
7. ICRP, Annex A. Radionuclides of the ICRP-07 collection. *Annals of the ICRP* **2008**, 38 (3), 35-96.
8. Veirs, D. K.; Worl, L. A.; Harradine, D. M.; Martinez, M. A.; Lillard, S.; Schwartz, D. S.; Puglisi, C. V.; Padilla, D. D.; Carrillo, A.; McInroy, R. E.; Montoya, A. R. *Gas generation and corrosion in salt-containing impure plutonium oxide materials: Initial results for ARF-102-85-223*; LA-UR-04-1788; Los Alamos National Laboratory: Los Alamos, NM, 2004.
9. Veirs, D. K.; Berg, J. M.; Stroud, M. A. *Obtaining G-values and rate constants from MIS data*; LA-UR-17-23787; Los Alamos National Laboratory: Los Alamos, NM, 2017.
10. Veirs, D. K.; Berg, J. M.; Crowder, M. L. *The effect of plutonium dioxide water surface coverage on the generation of hydrogen and oxygen*; LA-UR-12-22377; Los Alamos National Laboratory: Los Alamos, NM, 2012.
11. Worl, L., Berg, John, Bielinberg, Patricia, Carrillo, Alex, Martinez, Max, Montoya, Adam, Veirs, Kirk, Puglisi, Charles, Rademacher, Dave, Schwartz, Dan, Harradine, David, McInroy, Rhonda, Hill, Dallas, Prenger, Coyne, Steward, Jim *Shelf Life Surveillance for PuO<sub>2</sub> Bearing Materials FY04 Second Quarterly Report*; Los Alamos National Laboratory: 2004.
12. Brunauer, S.; Emmett, P. H.; Teller, E., Adsorption of Gases in Multimolecular Layers. *Journal of the American Chemical Society* **1938**, 60.
13. Farr, J. D.; Schulze, R. K.; Neu, M. P., Surface chemistry of Pu oxides. *Journal of Nuclear Materials* **2004**, 328, 124-136.
14. Veirs, D. K.; Berg, J. M.; Hill, D. D.; Harradine, D. M.; Narlesky, J. E.; Romero, E. L.; Trujillo, L.; Wilson, K. V. *Water radiolysis on plutonium dioxide: Initial results identifying a threshold relative humidity for oxygen gas generation*; LA-UR-12-26423; Los Alamos National Laboratory: Los Alamos, NM, 2012.
15. Sims, H. E. W., K. J.; Brown, J.; Morris, D.; Taylor, R. J., Hydrogen yields from water on the surface of plutonium dioxide. *Journal of Nuclear Materials* **2013**, (437), 359-364.
16. Haschke, J. M.; Ricketts, T. E., Adsorption of water on plutonium dioxide. *Journal of Alloys and Compounds* **1997**, 252, 148-156.

## Attachment 1: Gas Generation Partial Pressure Data and Uncertainties in kPa

Note: Total pressure values were reduced by 4kPa to correct for the estimated partial pressure of water vapor. Partial pressures were corrected for variation in the sensitivity of the GC with time. The average manifold background pressure was subtracted from the partial pressures.

Date	12/16/03	2/11/04	2/26/04	6/8/04	1/17/05	8/23/05	4/13/06	10/23/06	10/30/07	9/16/08	12/14/09	2/11/10	2/25/10
Days	0	57	72	175	398	616	849	1042	1414	1736	2190	2249	2263
CO <sub>2</sub>	0.0	17.4	18.9	25.5	28.5	28.8	29.4	28.3	26.8	23.4	14.5	14.6	14.3
N <sub>2</sub> O	0.0	5.8	4.8	1.4	0.6	0.6	0.6	0.7	0.7	0.7	0.8	0.8	0.8
He	71.2	70.0	68.6	68.1	68.8	74.2	69.6	69.4	68.7	65.4	64.3	67.7	66.0
H <sub>2</sub>	0.0	2.0	2.2	2.2	1.2	2.3	1.3	1.0	1.1	0.7	0.8	0.8	0.8
O <sub>2</sub>	1.9	0.4	0.6	0.7	0.3	0.1	0.1	0.1	0.1	0.5	1.3	0.1	0.1
N <sub>2</sub>	6.0	18.4	20.0	26.1	30.0	31.4	34.7	36.3	37.8	41.8	49.5	47.0	47.6
CH <sub>4</sub>	0.0	0.0	0.0	0.0	0.0	0.0	0.0	0.0	0.0	0.0	0.0	0.0	0.0
CO	0.0	3.8	4.2	3.5	1.2	0.8	0.7	0.7	0.6	0.5	0.6	0.4	0.5

### Uncertainties

Date	12/16/03	2/11/04	2/26/04	6/8/04	1/17/05	8/23/05	4/13/06	10/23/06	10/30/07	9/16/08	12/14/09	2/11/10	2/25/10
Days	0	57	72	175	398	616	849	1042	1414	1736	2190	2249	2263
CO <sub>2</sub>	0.00	0.65	0.69	0.88	1.04	1.12	1.09	1.08	1.00	0.90	0.60	0.52	0.53
N <sub>2</sub> O	0.00	0.23	0.19	0.07	0.03	0.04	0.04	0.04	0.05	0.05	0.05	0.04	0.01
He	2.86	2.44	2.40	2.37	2.37	2.47	2.33	2.30	2.30	2.15	2.26	2.57	2.50
H <sub>2</sub>	0.00	0.07	0.07	0.07	0.04	0.08	0.04	0.04	0.04	0.03	0.03	0.03	0.04
O <sub>2</sub>	0.09	0.02	0.03	0.04	0.02	0.02	0.02	0.01	0.02	0.04	0.07	0.02	0.01
N <sub>2</sub>	0.28	0.71	0.77	1.00	1.12	1.21	1.34	1.39	1.47	1.61	1.75	1.62	1.66
CH <sub>4</sub>	0.00	0.00	0.00	0.00	0.00	0.00	0.00	0.00	0.00	0.00	0.00	0.00	0.00
CO	0.00	0.16	0.17	0.15	0.06	0.05	0.04	0.04	0.04	0.03	0.04	0.03	0.03

## Attachment 2 Gas Generation: Total Pressure

Date	Pressure (kPa)	Date	Pressure (kPa)	Date	Pressure (kPa)	Date	Pressure (kPa)	Date	Pressure (kPa)
		6/28/2004	126.4	1/17/2005	130.7	8/8/2005	136.9	4/10/2006	136.2
12/15/2003	76.7	7/5/2004	126.6	1/24/2005	129.5	8/15/2005	136.9	4/17/2006	135.0
12/22/2003	88.1	7/12/2004	126.9	1/31/2005	130.1	8/22/2005	137.3	4/24/2006	134.9
12/29/2003	95.4	7/19/2004	127.4	2/7/2005	130.4	8/29/2005	136.2	5/1/2006	134.5
1/5/2004	100.8	7/26/2004	127.4	2/14/2005	131.1	9/5/2005	135.9	5/8/2006	134.6
1/12/2004	105.3	8/2/2004	127.4	2/21/2005	131.2	9/12/2005	135.6	5/15/2006	134.5
1/19/2004	108.6	8/9/2004	127.7	2/28/2005	131.6	9/19/2005	135.7	5/22/2006	134.9
1/26/2004	111.8	8/16/2004	127.7	3/7/2005	132.0	9/26/2005	135.5	5/29/2006	
2/2/2004	114.3	8/23/2004	127.9	3/14/2005	131.8	10/3/2005	135.4	6/5/2006	135.0
2/9/2004	116.0	8/30/2004	127.7	3/21/2005	131.8	10/10/2005	135.1	6/12/2006	135.0
2/16/2004	116.5	9/6/2004	127.7	3/28/2005	131.7	10/17/2005	134.9	6/19/2006	135.0
2/23/2004	118.1	9/13/2004	128.0	4/4/2005	131.8	10/24/2005	134.7	6/26/2006	135.2
3/1/2004	118.2	9/20/2004	128.2	4/11/2005	131.8	10/31/2005	134.3	7/3/2006	134.8
3/8/2004	119.3	9/27/2004	128.1	4/18/2005	131.9	11/7/2005	134.7	7/10/2006	134.6
3/15/2004	120.3	10/4/2004	128.2	4/25/2005	131.9	11/14/2005	134.3	7/17/2006	
3/22/2004	121.6	10/11/2004	128.5	5/2/2005	132.1	11/21/2005	134.0	7/24/2006	134.6
3/29/2004	122.5	10/18/2004	128.7	5/9/2005	132.7	11/28/2005	133.7	7/31/2006	134.8
4/5/2004	122.7	10/25/2004	128.7	5/16/2005	132.8	12/5/2005	133.6	8/7/2006	134.8
4/12/2004	123.4	11/1/2004	128.7	5/23/2005	132.7	12/12/2005	133.8	8/14/2006	135.3
4/19/2004	122.9	11/8/2004	129.0	5/30/2005	132.9	12/19/2005	133.7	8/21/2006	135.0
4/26/2004	123.1	11/15/2004	129.5	6/6/2005	133.1	12/26/2005	133.6	8/28/2006	135.0
5/3/2004	124.8	11/22/2004	129.6	6/13/2005	133.3	1/2/2006	133.3	9/4/2006	135.1
5/10/2004	125.1	11/29/2004	129.8	6/20/2005	133.4	1/9/2006	133.2	9/11/2006	135.1
5/17/2004	125.4	12/6/2004	130.2	6/27/2005	135.3	1/16/2006	133.6	9/18/2006	135.2
5/24/2004	125.6	12/13/2004	130.4	7/4/2005	135.7	1/23/2006	134.3	9/25/2006	135.1
5/31/2004	125.8	12/20/2004	130.5	7/11/2005	135.9	1/30/2006	134.1	10/2/2006	135.1
6/7/2004	126.2	12/27/2004	130.4	7/18/2005	135.8	2/6/2006	134.0	10/9/2006	135.2
6/14/2004	125.3	1/3/2005	130.6	7/25/2005	136.4	2/13/2006	134.3	10/16/2006	135.8
6/21/2004	125.8	1/10/2005	130.6	8/1/2005	136.6	2/20/2006	134.7	10/23/2006	135.2

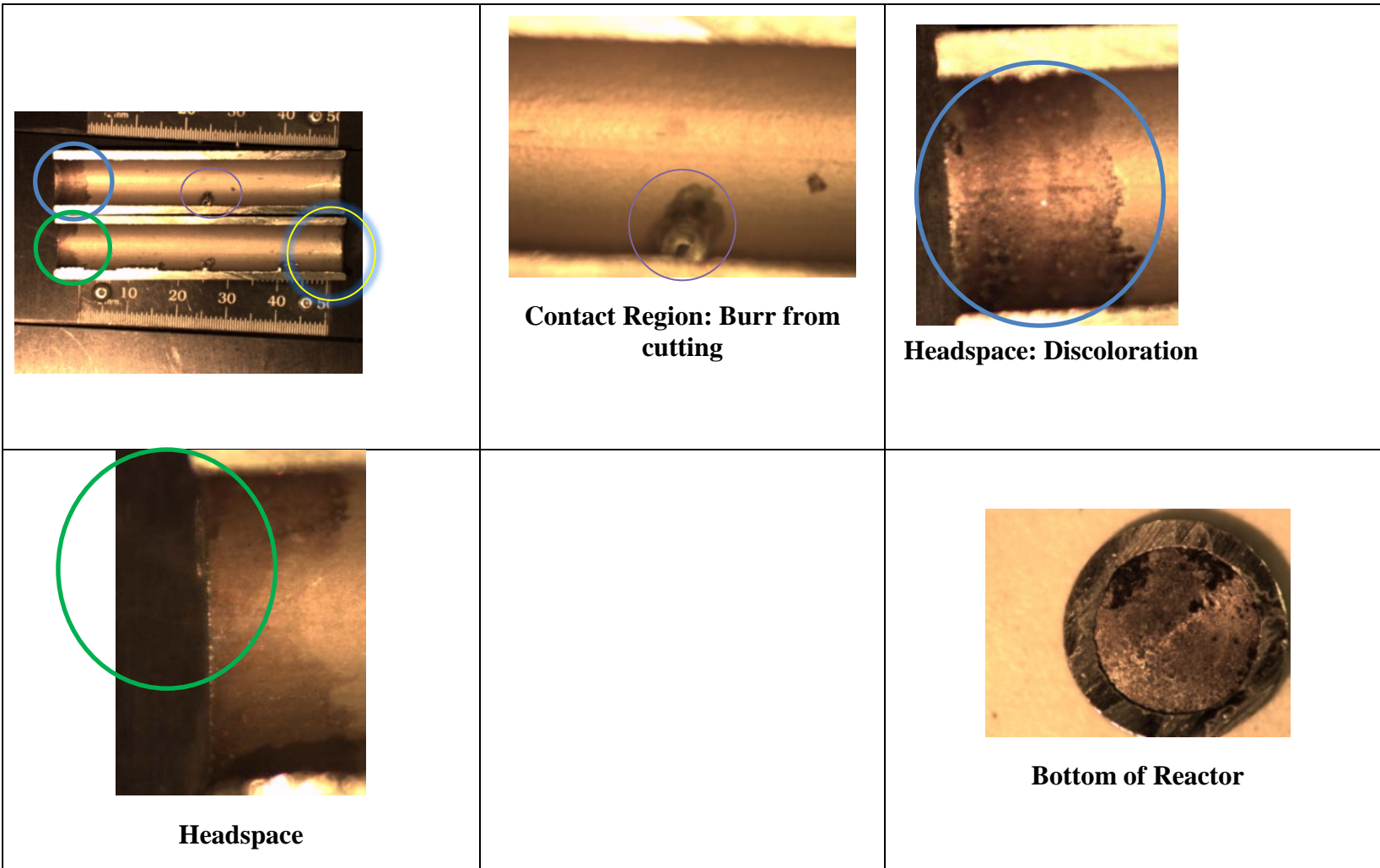
**Attachment 2 Gas Generation: Total Pressure (cont.)**

Date	Pressure (kPa)	Date	Pressure (kPa)						
10/30/2006	135.4	6/4/2007	136.3	12/24/2007	133.4	7/14/2008	135.4	2/2/2009	132.2
11/6/2006	135.6	6/11/2007	136.4	12/31/2007	133.2	7/21/2008	135.1	2/9/2009	132.2
11/13/2006	115.7	6/18/2007	136.5	1/7/2008	133.3	7/28/2008	135.4	2/16/2009	132.6
11/20/2006	136.0	6/25/2007	136.6	1/14/2008	133.1	8/4/2008	135.6	2/23/2009	132.6
11/27/2006	136.0	7/2/2007	136.4	1/21/2008	133.3	8/11/2008	135.3	3/2/2009	132.4
12/4/2006	136.0	7/9/2007	136.3	1/28/2008	133.1	8/18/2008	135.2	3/9/2009	132.5
12/11/2006	136.0	7/16/2007	136.4	2/4/2008	132.8	8/25/2008	135.2	3/16/2009	132.6
12/18/2006	136.1	7/23/2007	136.2	2/11/2008	132.8	9/1/2008	134.9	3/23/2009	132.8
12/25/2006	135.9	7/30/2007	136.4	2/18/2008	133.2	9/8/2008	134.4	3/30/2009	132.8
1/1/2007	135.9	8/6/2007	135.7	2/25/2008	133.3	9/15/2008	134.0	4/6/2009	132.9
1/8/2007	136.3	8/13/2007	135.6	3/3/2008	133.2	9/22/2008	132.4	4/13/2009	132.8
1/15/2007	136.2	8/20/2007	135.8	3/10/2008	132.9	9/29/2008	132.2	4/20/2009	132.6
1/22/2007	136.1	8/27/2007	135.9	3/17/2008	133.3	10/6/2008	131.9	4/27/2009	132.5
1/29/2007	136.3	9/3/2007	136.0	3/24/2008	133.6	10/13/2008	131.9	5/4/2009	132.6
2/5/2007	136.1	9/10/2007	135.9	3/31/2008	133.6	10/20/2008	131.8	5/11/2009	132.8
2/12/2007	136.0	9/17/2007	135.7	4/7/2008	133.7	10/27/2008	131.8	5/18/2009	132.7
2/19/2007	136.2	9/24/2007	135.9	4/14/2008	133.9	11/3/2008	131.8	5/25/2009	133.1
2/26/2007	136.2	10/1/2007	135.6	4/21/2008	133.8	11/10/2008	131.6	6/1/2009	133.5
3/5/2007	136.5	10/8/2007	135.2	4/28/2008	134.1	11/17/2008	131.6	6/8/2009	133.6
3/12/2007	136.6	10/15/2007	135.6	5/5/2008	136.0	11/24/2008	131.8	6/15/2009	132.6
3/19/2007	136.6	10/22/2007	135.5	5/12/2008	135.8	12/1/2008	131.8	6/22/2009	132.6
3/26/2007	136.6	10/29/2007	135.4	5/19/2008	135.9	12/8/2008	131.8	6/29/2009	132.2
4/2/2007	136.4	11/5/2007	133.6	5/26/2008	136.1	12/15/2008	132.1	7/6/2009	132.0
4/9/2007	136.1	11/12/2007	133.3	6/2/2008	136.0	12/22/2008	132.1	7/13/2009	131.9
4/16/2007	136.0	11/19/2007	133.6	6/9/2008	136.3	12/29/2008	132.4	7/20/2009	131.7
4/23/2007	136.0	11/26/2007	133.1	6/16/2008	136.0	1/5/2009	132.3	7/27/2009	132.0
4/30/2007	136.1	12/3/2007	133.3	6/23/2008	135.8	1/12/2009	132.0	8/3/2009	131.9
5/21/2007	136.3	12/10/2007	133.4	6/30/2008	136.0	1/19/2009	132.1	8/10/2009	131.8
5/28/2007	136.3	12/17/2007	133.9	7/7/2008	135.5	1/26/2009	132.1	8/17/2009	131.9

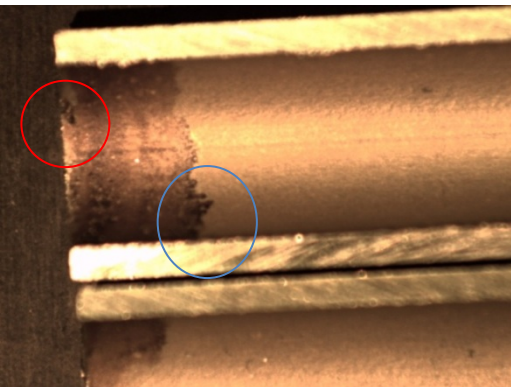
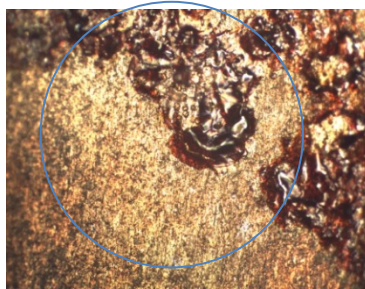
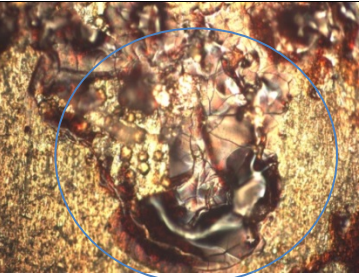
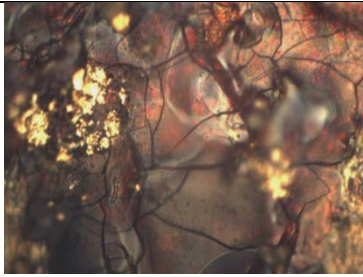
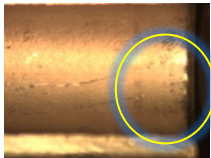
## Attachment 2 Gas Generation: Total Pressure (cont.)

Date	Pressure (kPa)	Date	Pressure (kPa)
8/24/2009	132.0	12/7/2009	132.2
8/31/2009	132.0	12/14/2009	132.0
9/7/2009	131.8	12/21/2009	130.8
9/14/2009	131.5	12/28/2009	130.8
9/21/2009	132.6	1/4/2010	130.6
9/28/2009	132.5	1/11/2010	130.7
10/5/2009	132.6	1/18/2010	130.7
10/12/2009	132.5	1/25/2010	130.6
10/19/2009	132.5	2/1/2010	130.5
10/26/2009	132.4	2/8/2010	130.1
11/2/2009	132.3	2/15/2010	129.6
11/9/2009	132.4	2/22/2010	129.6
11/16/2009	132.6	3/1/2010	128.1
11/23/2009	132.4		
11/30/2009	132.3		

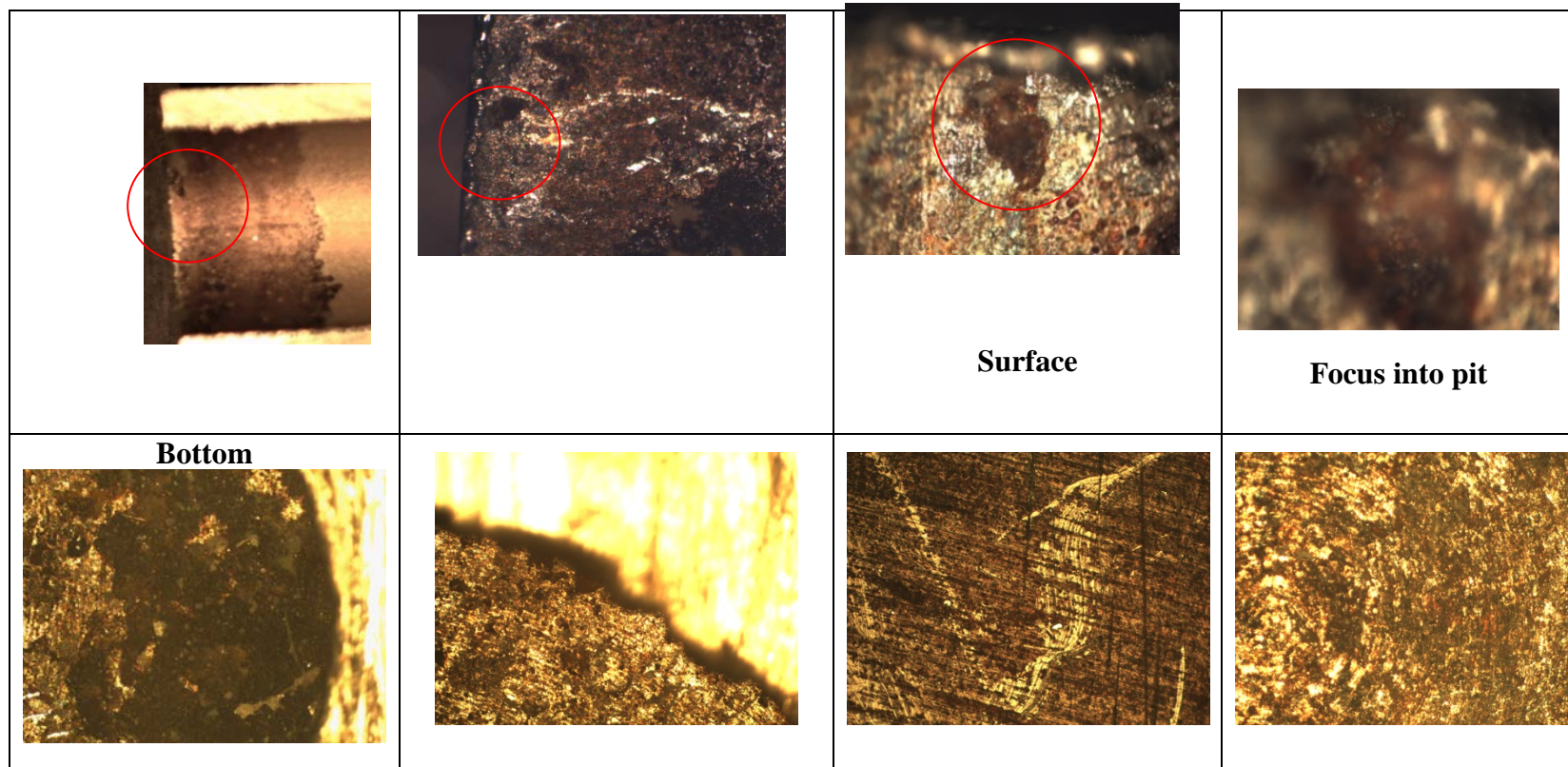
### Attachment 3 Photographs of the SSR inner bucket



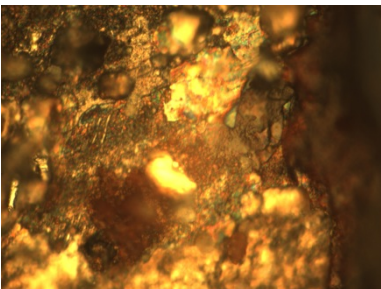
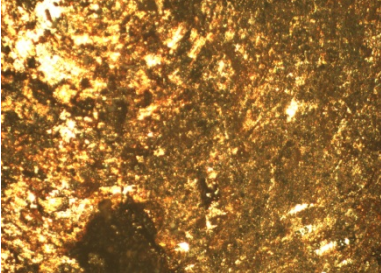
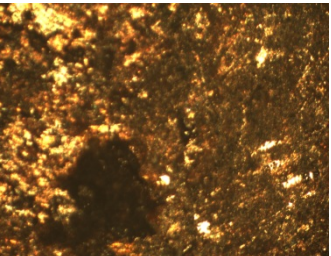
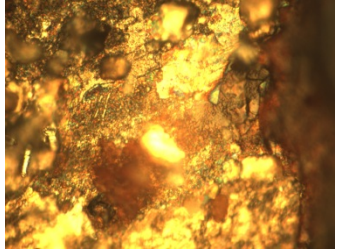
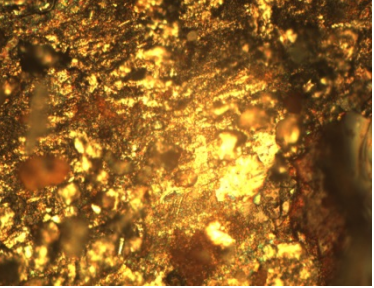
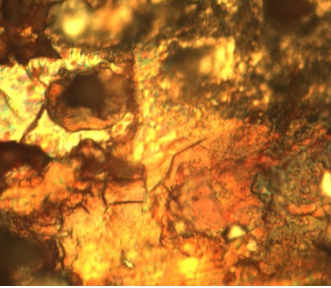
**Attachment 3 Photographs of the SSR inner bucket (continued)**

			
	<b>Interface</b>	<b>Interface</b>	
			
<b>Interface</b>	<b>Interface</b>		
			
<b>Contact Region</b>	<b>Contact Region</b>	<b>Contact Region: Machining Marks</b>	<b>Contact Region: Debris/no pits</b>

**Attachment 3 Photographs of the SSR inner bucket (continued)**



**Attachment 3 Photographs of the SSR inner bucket (continued)**

<b>Bottom</b> 			
<b>Bottom</b> 			

## Appendix 1: Estimating the monolayer coverage

**Surface Area:** The number of monolayers of moisture on the sample surface may be calculated if the mass of moisture or water, the mass of the sample, and the SSA of the sample are known. One approach is to determine the weight percentage for one monolayer of water. The number of monolayers of water can be calculated by dividing the total weight percentage of water (mass of water/mass of the sample) by the weight percentage of one monolayer of water.<sup>16</sup> The weight percentage of one monolayer of water is the product of the weight of water in a monolayer of 1 m<sup>2</sup> and the SSA:

$$\begin{aligned} \text{wt\% of 1 ML} &= 0.00022 \text{ g m}^{-2} \text{ML}^{-1} \times \text{SSA m}^2 \text{ g}^{-1} \times 100 \text{ wt\%} \\ &= 0.022 \text{ wt\% ML}^{-1} \times \text{SSA.} \end{aligned} \quad \text{Equation A1-1}$$

For the material TS707001 with a SSA of 2.346 m<sup>2</sup> g<sup>-1</sup>, the weight percentage of one monolayer of water is 0.052 wt% ML<sup>-1</sup>.

Dividing the weight percentage of water by the weight percentage of water in one monolayer yields the number of monolayers of water. Applying this to the measured weight percentage of water upon loading and unloading results in:

$$\text{Loading Condition: } 0.27 \text{ wt\%} / 0.052 \text{ wt\% ML}^{-1} = 5.2 \text{ ML}$$

$$\text{Unloading Condition: } 0.11 \text{ wt\%} / 0.052 \text{ wt\% ML}^{-1} = 2.1 \text{ ML}$$

**BET Theory:** The number of monolayers can also be estimated based upon the relative humidity in the container using Brunauer-Emmett-Teller (BET) theory.<sup>12</sup> BET theory is the standard model for quantifying the equilibria between multiple physically adsorbed layers on a surface and the adsorbing species in the gas above the surface. The specific relationship between the RH above a surface and the number of monolayers of weakly bound water on the surface predicted by BET theory is illustrated in Fig. A-1.

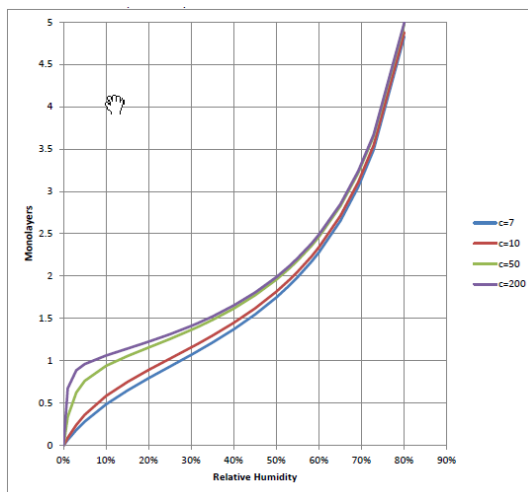


**Figure A-1. Adsorption Isotherm Calculated from BET Theory.**

## Appendix 2: Stopping power ratio

The ratio of the stopping power due to the water and the stopping power due to the material is calculated using the approach in Appendix B of Reference 6.

Species	Integrated at 5.2MeV		TS707001	
H <sub>2</sub> O(g)	7.946			
H <sub>2</sub> O (l)	7.708			
F	6.645		0.0000	0
O	5.901		0.0000	0
Na	5.304		0.0000	0
C	5.190		0.0000	0
S	5.117		0.0000	0
Mg	5.100		0.0000	0
Si	4.852		0.0000	0
Al	4.702		0.0000	0
K	4.652		0.0000	0
Cl	4.575		0.0000	0
Ca	4.461		0.0000	0
Cr	3.688		0.0000	0
Fe	3.504		0.0000	0
Ni	3.184		0.0000	0
Cu	2.871		0.0000	0
Zn	2.860		0.0000	0
Ga	2.786		0.0000	0
UO <sub>2</sub>	2.081		1.0000	2.080943

S <sub>mat</sub>	2.080943
S <sub>water</sub>	7.708
S	3.704089